Supplementary Figure S1

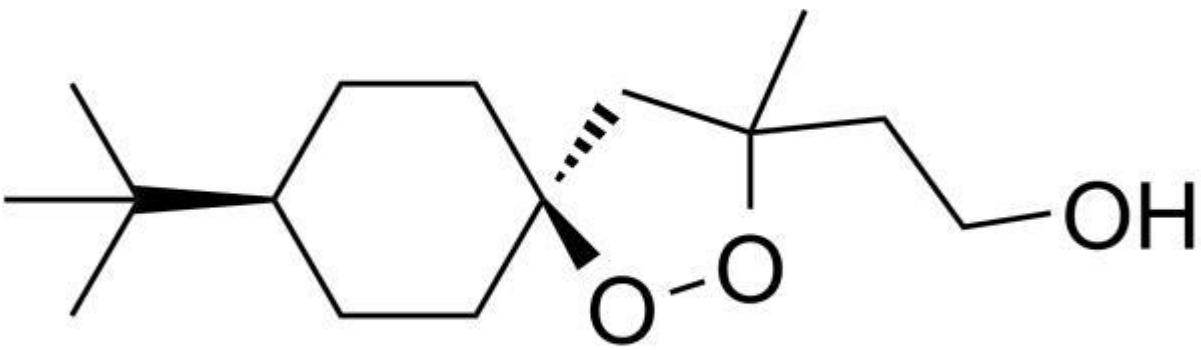

Supplementary Figure S1. The chemical structure of $FINO_2$.

Supplementary Figure S2

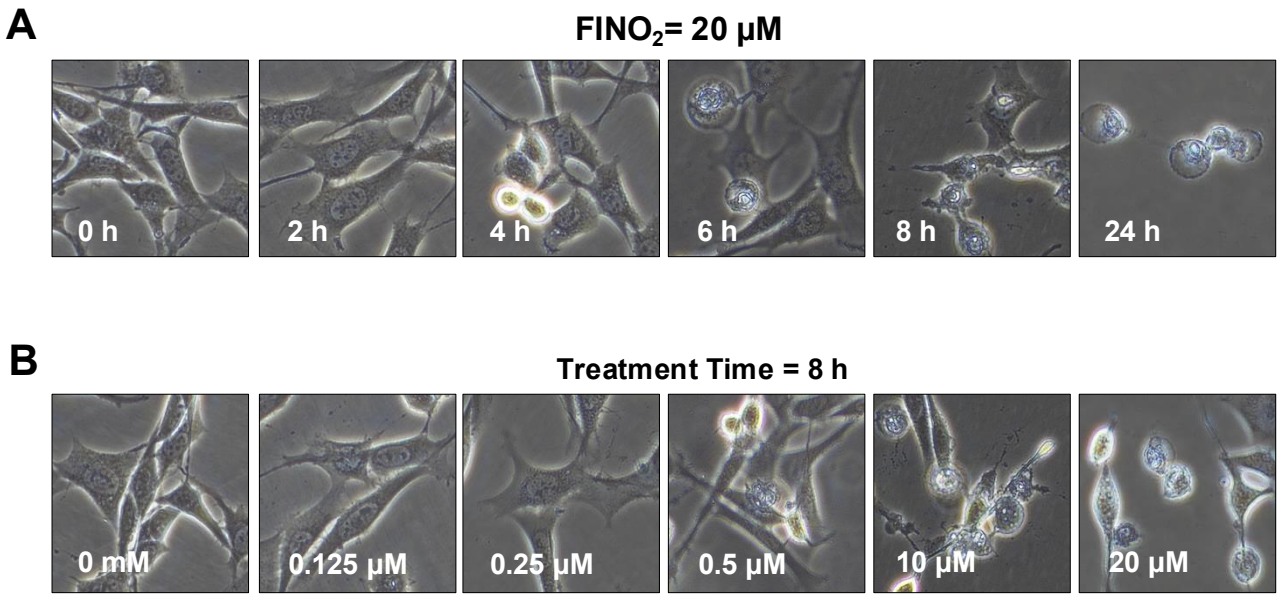

Supplementary Figure S2. Time- and dose-dependent induction of ferroptotic cell death by $FINO_2$ in HT22 cells

A. Time- dependent induction of cell death by $FINO_2$ in cells. Cells were treated with 20 μM $FINO_2$ for 0, 2, 4, 6, 8 and 24 h. changed in gross morphology (light microscope, 40×, scale bar = 100 μm).

B. Does- dependent induction of cell death by $FINO_2$ in cells. Cells were treated with different concentrations of $FINO_2$ for 24 h changed in gross morphology (light microscope, 40×, scale bar = 100 μm).

Supplementary Figure S3

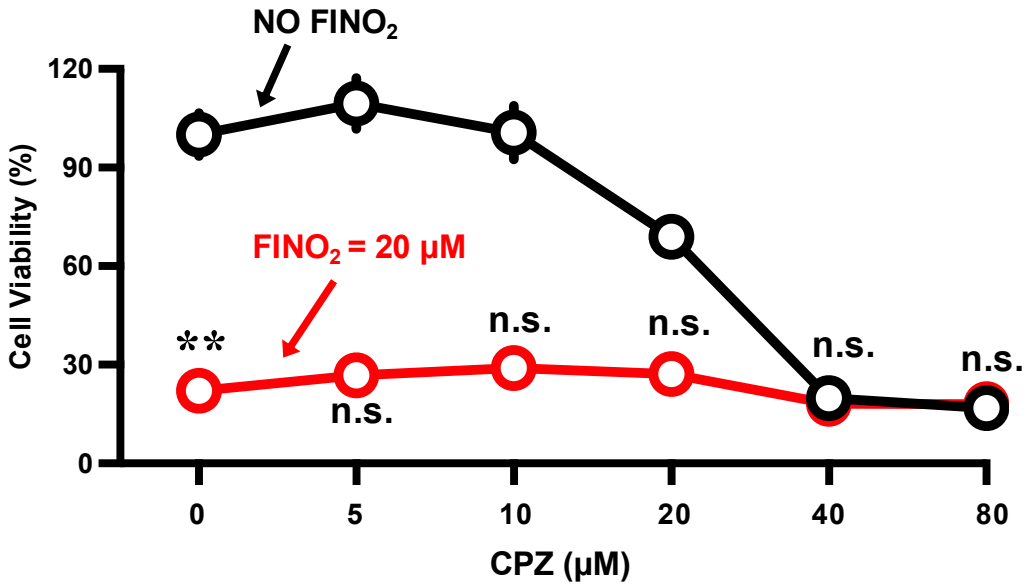

Supplementary Figure S3. Effects of CPZ on $FINO_2$-induced ferroptosis in HT22 cells.

Protective effect of CPZ against $FINO_2$-induced cytotoxicity in cells. Cells were treated with $FINO_2$ (20 μM) ± CPZ (5, 10, 20, 40 and 80 μM) for 24 h, and then subjected to MTT assay (n = 4). Quantitative data are presented as mean ± S.D. ** $P < 0.01$; n.s., not significant.

Supplementary Figure S4

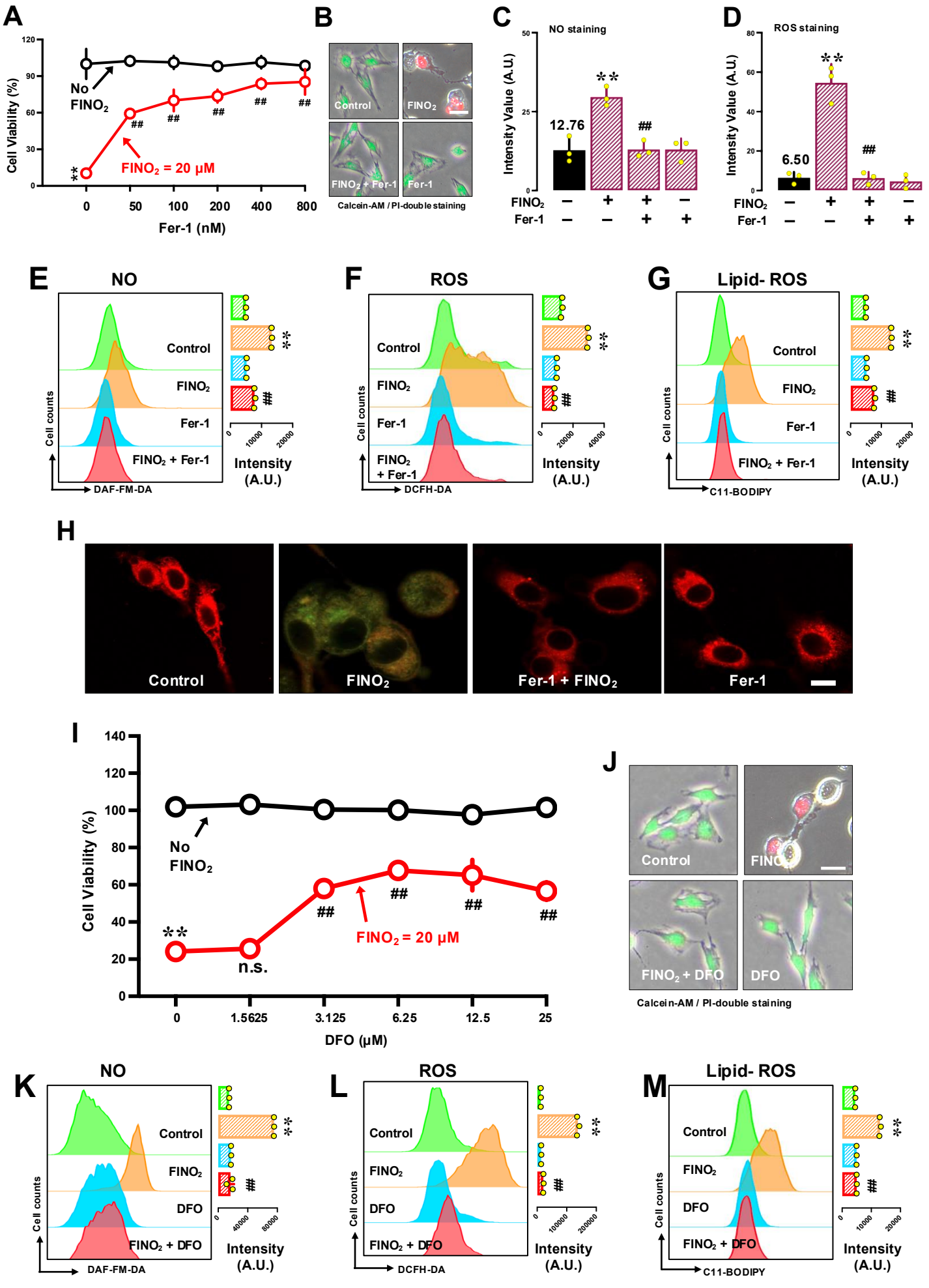

Supplementary Figure S4. Effects of Fer-1 and DFO on $FINO_2$-induced ferroptosis and on the accumulation of NO, ROS and lipid-ROS in HT22 cells.

A, B. Protective effect of Fer-1 against $FINO_2$-induced cytotoxicity. In **A**, cells were treated with $FINO_2$ (20 μM) ± Fer-1 (25, 50, 100, 200, 400 and 800 nM) for 24 h, and then subjected to MTT assay (n = 4). In B, cells were treated with $FINO_2$ (20 μM) ± Fer-1 (400 nM) for 24 h, and then subjected to fluorescent microscopy following Calcein-AM/PI staining (green for live cells, and red for dead cells; scale bar = 100 μm).

C–H. Abrogation by Fer-1 of $FINO_2$-induced accumulation of cellular NO (**C, E**), ROS (**D, F**) and lipid-ROS (**G, H**). Cells were treated with $FINO_2$ (20 μM) ± Fer-1 (400 nM) for 8 h, and then subjected to fluorescence microscopy (**C, D**), analytical flow cytometry (**E–G**), and confocal microscopy (**H**; scale bar = 100 μm). For data in **C**, **D**, only quantitative intensity values are shown (n = 3; the mean value for the control group is shown on top of the bar); for flow cytometry data (**E–G**), the left panels are the histograms, and the right panels are the quantitative values (n = 3).

I, J. Protective effect of DFO against $FINO_2$-induced cytotoxicity. In **I**, cells were treated with $FINO_2$ (20 μM) ± DFO (1.5825, 3.125, 6.25, 12.5 and 25 μM) for 24 h, and then subjected to MTT assay (n = 4). In **J**, cells were treated with $FINO_2$ (20 μM) ± DFO (6.25 μM) for 24 h, and then subjected to fluorescence microscopy following Calcein-AM/PI staining (green for live cells, and red for dead cells; scale bar = 100 μm).

K–M. Partial abrogation by DFO of $FINO_2$-induced accumulation of cellular NO (**K**), ROS (**L**) and lipid-ROS (**M**). Cells were treated with $FINO_2$ (20 μM) ± DFO (6.25 μM) for 8 h, and then subjected to analytical flow cytometry. For flow cytometry data (**K–M**), the left panels are the histograms, and the right panels are the quantitative values (n = 3).

Quantitative data are presented as mean ± S.D. ** or $^{\#\#}$ $P < 0.01$; n.s., not significant.

Supplementary Figure S5

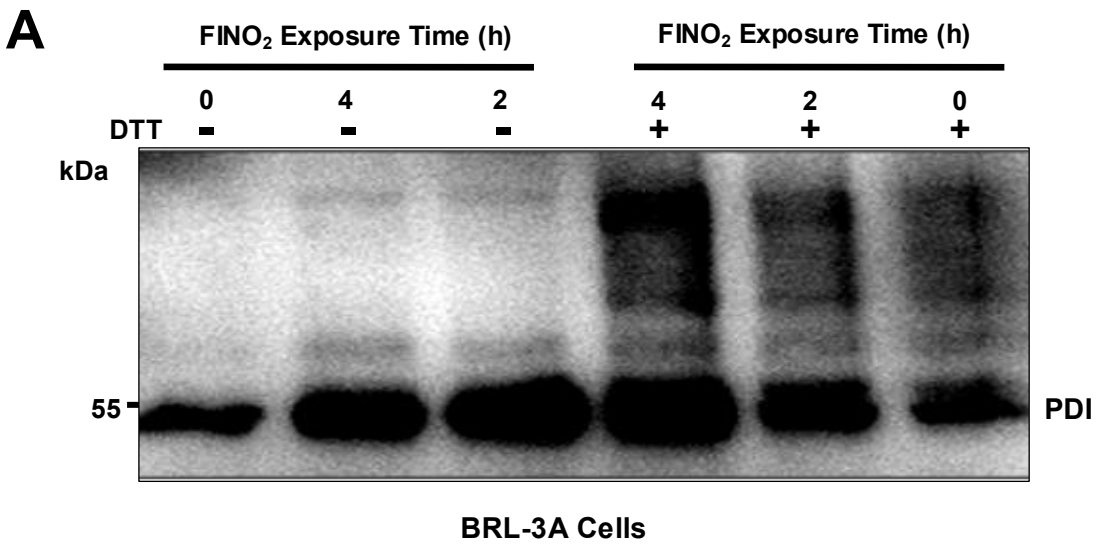

Supplementary Figure S5. Effect of $FINO_2$ exposure on PDI thiol redox state in HT22 cells.

A. The thiol redox state was determined using mPEG-maleimide mobility-shift (PEG-switch) assay under both nonreducing (−DTT) and reducing (+DTT) conditions following FINO2 exposure for 0, 2 and 4 h.

Supplementary Figure S6

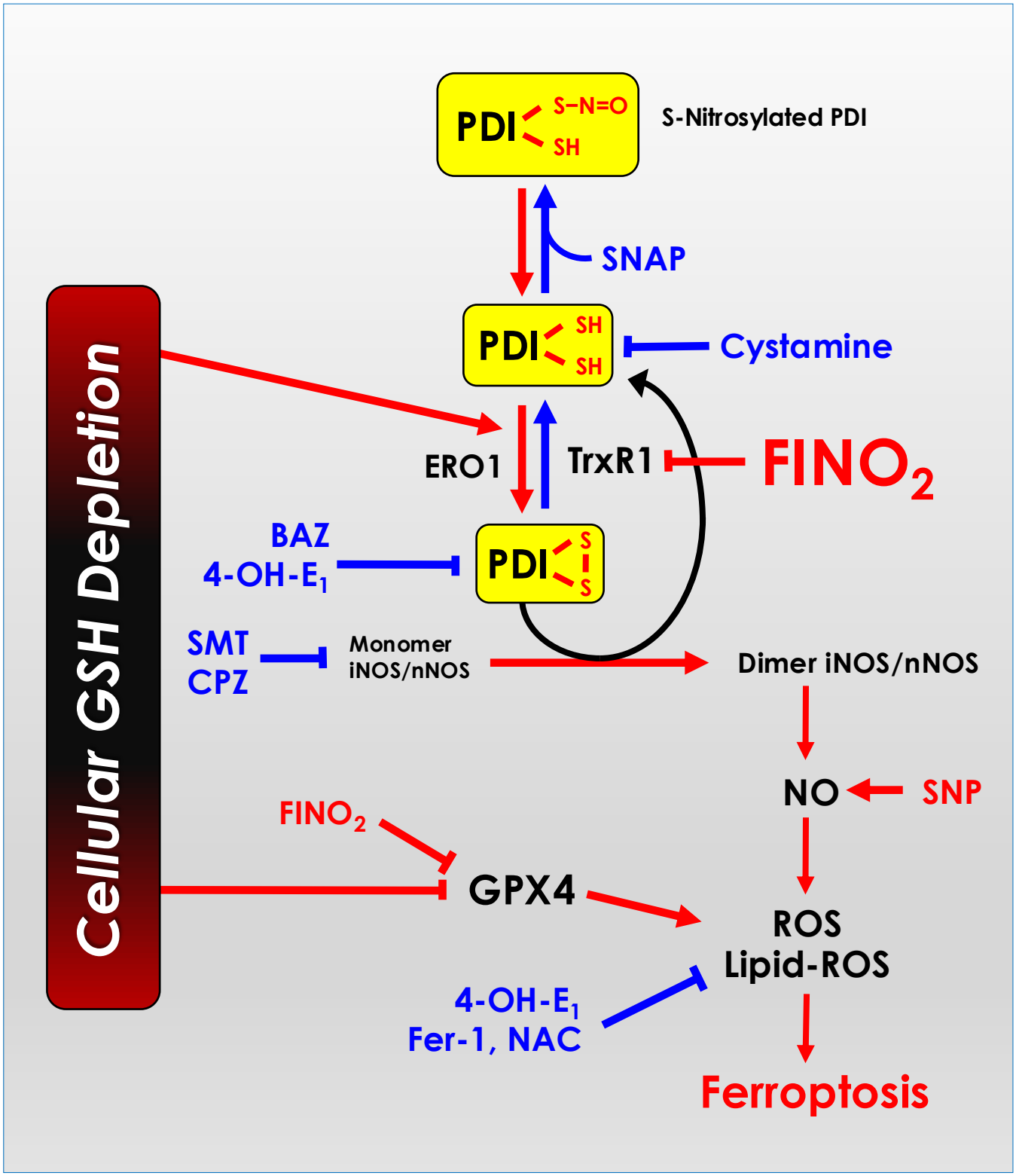

Supplementary Figure S6. Schematic depiction of the role of PDI–NOS–NO–ROS/lipid-ROS in mediating $FINO_2$-induced ferroptosis. For details, please refer to the **DISCUSSION** section.